Supporting Information

for *Adv. Mater.*, DOI: 10.1002/adma.((please add manuscript number))

High-performance Doped Silver Films: Overcoming Fundamental Material Limits for Nanophotonic Applications

*Cheng Zhang, Nathaniel Kinsey, Long Chen, Chengang Ji, Mingjie Xu, Marcello Ferrera, Xiaoqing Pan, Vladimir M. Shalaev, Alexandra Boltasseva and L. Jay Guo**

1. Thin Silver film

1.1 Thin Ag film degradation in air

While a 15 nm as-deposited pure Ag film has a continuous surface morphology (figure SI-1a), it will degrade rapidly in the ambient environment. This is due to the aggregation of Ag atoms, which is shown in the SEM picture taken 30 minutes after the sample being taken out of the deposition chamber (Figure SI-1b).

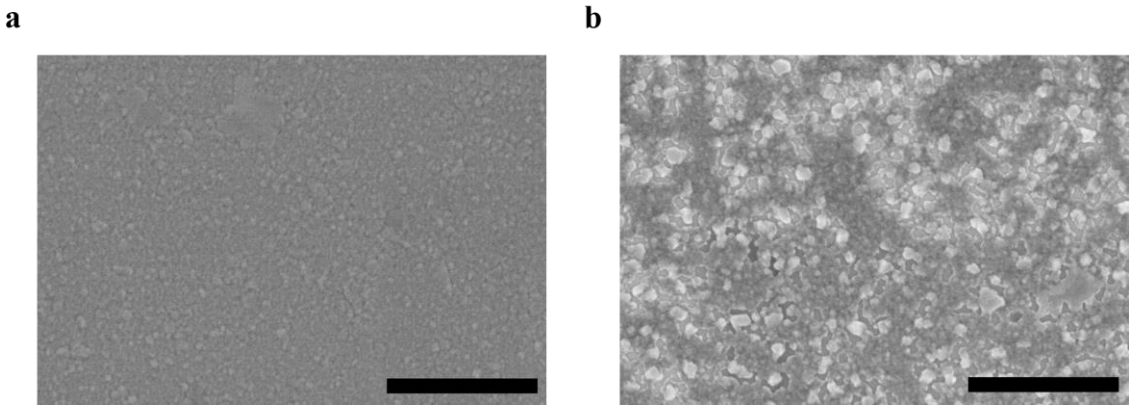

Figure SI-1. a) SEM of a 15-nm fresh pure Ag film on fused silica substrate. b) SEM of a 15-nm pure Ag film on fused silica substrate 30 minutes after the deposition, and the Ag atoms have aggregated to form islands. The scale bar is 1 μm.

1.2 De-wetting of Ag films under elevated temperatures

Pure Ag films are known to have a poor thermal stability. For example, a 30 nm thick Ag films form islands after being annealed in N_2 environment at 300 °C for 3 minutes (Figure SI-2). In contrast, Al-doped Ag film can withstand annealing up to 500 °C without scarifying its smooth morphology.

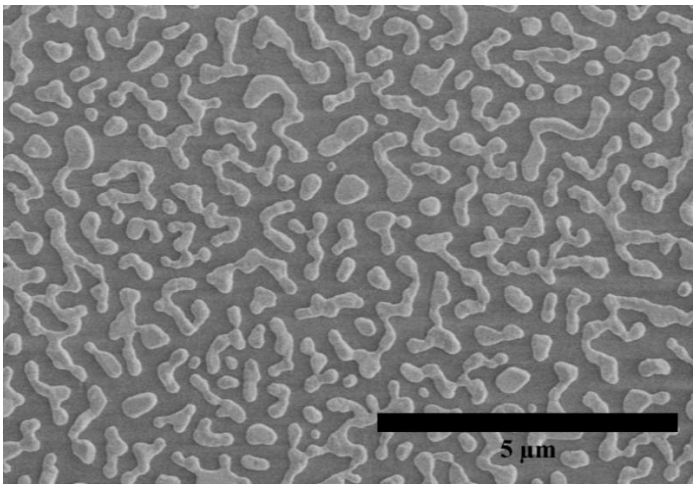

Figure SI-2. SEM picture of a 30 nm Ag film underwent annealing in N_2 environment at 300 °C for 3 minutes. The film has totally de-wetted from the fused silica substrate.

1.3 Dis-continuous thin Ag film

Ag follows the Volmer-Weber (3D) growth mode during the vacuum deposition, where the Ag atoms tend to aggregate into isolated islands. As the deposition continues, these islands eventually connect with each other to form a semi-continuous/conductive film. Consequently, thin Ag films below 10 nm are known to be discontinuous and consequently have very rough surface morphologies. We characterized the surface morphology of a 7-nm pure Ag (nominal thickness) film using Atomic Force Microscope (AFM), and the film is shown to have a rough surface with RMS roughness of 4.9 nm (figure SI-3).

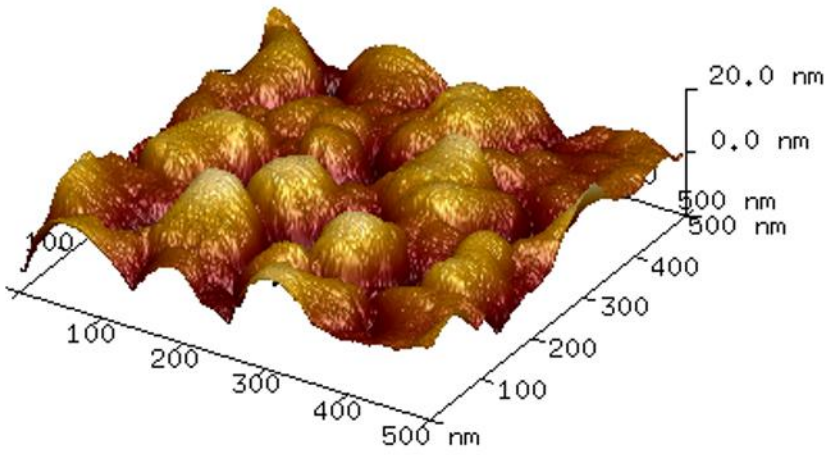

Figure SI-3. AFM image of a 7-nm (nominal thickness) Ag film on fused silica substrate. The film is dis-continuous and has a RMS roughness of 4.9 nm.

2. Thin Aluminum-doped Silver film

2.1 Long term stability of Al-doped Ag in air

In contrast, Al-doped Ag films have a significantly improved stability in air compared with pure thin Ag films. Figure SI-4 shows the pictures of a freshly deposited Al-doped Ag film on fused silica substrate (left), and another sample which has been 6 months after deposition (right). Both films show uniform and similar appearances.

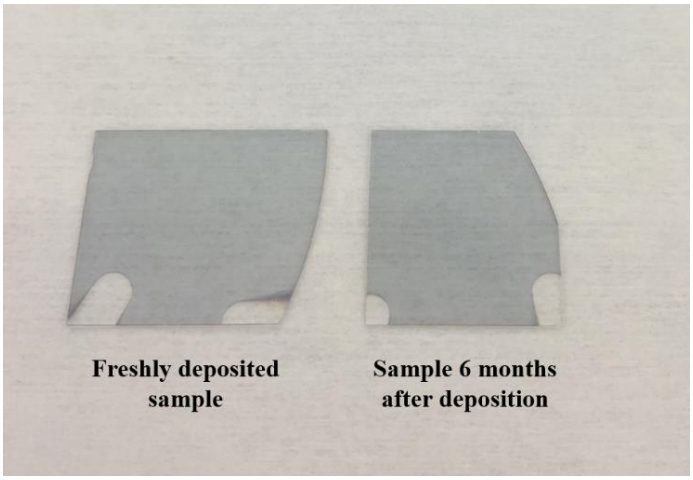

Figure SI-4. Pictures of a freshly deposited Al-doped Ag film on fused silica substrate (left), and another sample which has been exposed to ambient environment for 6 months (right). Both films show uniform and similar appearances.

2.2 Thermal stability of Al-doped Ag films

While the pure Ag film forms islands after annealing (Figure S3), the Al-doped Ag film maintains its smooth surface morphology. Figure SI-5 shows the AFM images of an as-deposited 7 nm Al-doped Ag film (a), and a 7 nm Al-doped Ag film underwent heating in N_2 at 500˚C for 3 minutes (b). The measured RMS roughness changes from 0.773 nm to 0.836 nm after the annealing treatment.

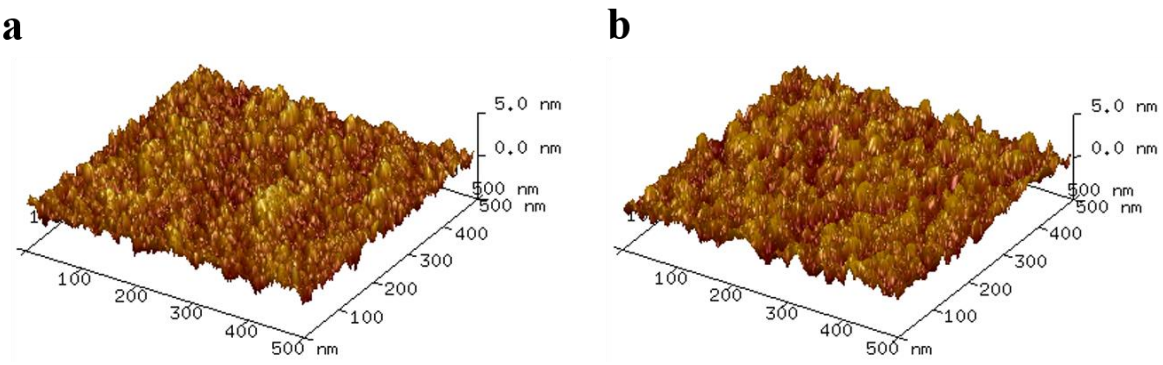

Figure SI-5. AFM images of an as-deposited 7 nm Al-doped Ag film (a), and a 7 nm Al-doped Ag film underwent heating in N_2 at 500˚C for 3 minutes (b). The measured RMS roughness changes from 0.773 nm to 0.836 nm after the annealing treatment.

3. Reflectance from thick Al-doped Ag and Ag films

One way to characterize the plasma frequency ω_p of a metal film is to measure its reflection spectrum. There will be a reflection dip near the ω_p. We experimentally characterized ω_p of 150 nm thick Al-doped Ag and Ag films by measuring their reflection spectra at at an angle of incidence of 45° using spectroscopic ellipsometer (M-2000DI, Woollam, Inc.). There is an 18 nm blue-shift of ω_p for Al-doped Ag compared to pure Ag (from 318 nm to 300 nm). Ag has one free electron per atom, while Al has three. Adding Al into Ag increases the density of free electrons, and thus, modify the plasma frequency of the resultant film. Our measurement corresponds well with a previous study, where the plasma frequency of 500 nm thick Al-Ag alloy film is characterized by the dip of the normal reflection spectra, and there is a blue shift in ω_p with the increase of Al concentration.

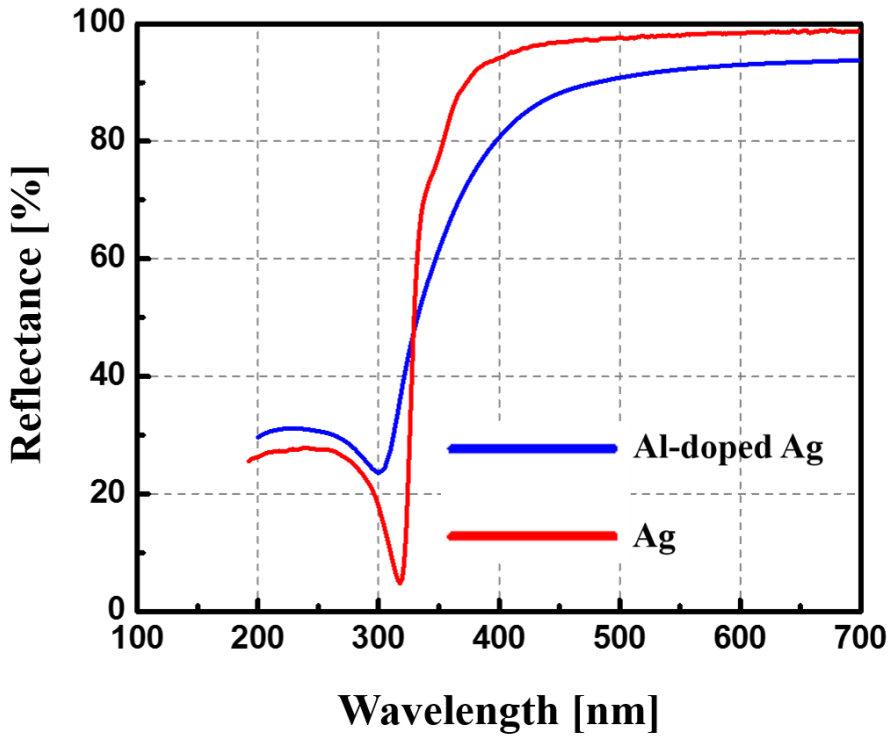

Figure SI-6. Measured reflection intensity from 150 nm thick Al-doped Ag and Ag films. There is an 18 nm blue-shift of ω_p for Al-doped Ag compared to pure Ag (from 318 nm to 300 nm), due to the doping of Al and the increased density of free electrons.

4. Film thickness determined by spectroscopic ellipsometry

The film thickness and refractive index are characterized by a spectroscopic ellipsometer before the bright field TEM characterization. The measurement procedure is explained in the Experimental Section. The fitting error of the ellipsometery measurement as a function of film thickness is plotted in figure SI-7. There is a minimized fitting error at a film thickness of 7.15 nm. This value corresponds well to the thickness characterized by the bright field TEM (figure 2a in the manuscript).

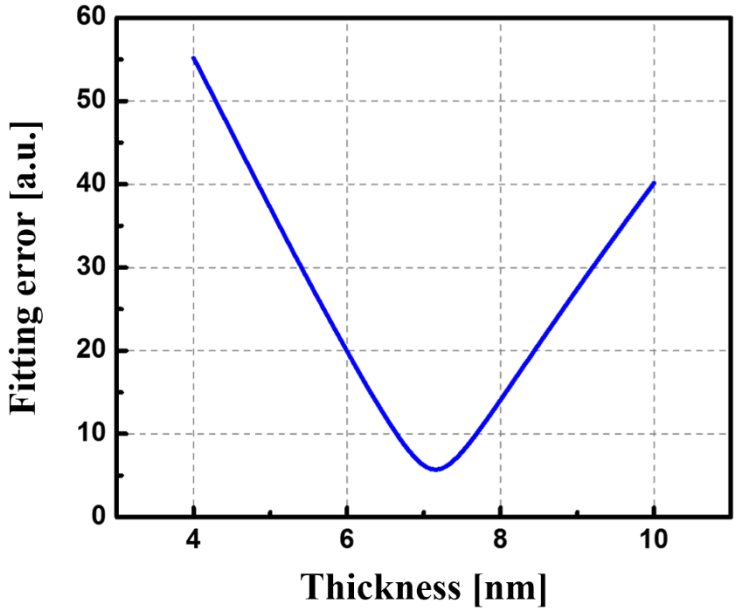

Figure SI-7. Fitting error of ellipsometry measurement as a function of the film thickness. The ellipsometry measurement has a lowest fitting error at the film thickness of 7.15 nm. The measured thickness by ellipsometry corresponds well to the thickness value determined by the bright field TEM.

5. Hyperbolic metamaterials (HMMs)

5.1 HMM dispersion curve and the propagation of high-k modes

The dispersion relation of HMMs is given by: $k_x^2/\varepsilon_\perp + k_z^2/\varepsilon_\parallel = k_0^2$, where k_x and k_z are the complex amplitudes of the transverse and normal components of the complex wave-vector, and k_0 is the free-space wave-vector (with respect to the coordinate system in Figure 2a). Since $\varepsilon'_\parallel < 0$ and $\varepsilon'_\perp > 0$, HMMs are governed by hyperbolic iso-frequency curves. For example, in the case of the HMM studied in this paper, the measured $\varepsilon'_\parallel$ and $\varepsilon'_\perp$ at 700 nm are -1.41529 and 7.86797 respectively. This leads to a dispersion curve shown in Figure SI-8. There is a cut-off band defined by $|k_x| < k_c$, where $k_c = \sqrt{\varepsilon_\perp} * k_0$. Electromagnetic waves with transverse wave-vector k_x located within this band decay evanescently in the normal direction. In contrast, for electromagnetic waves with transverse wave-vectors $|k_x| > k_c$, they are allowed to propagate in the HMM (high-k modes).

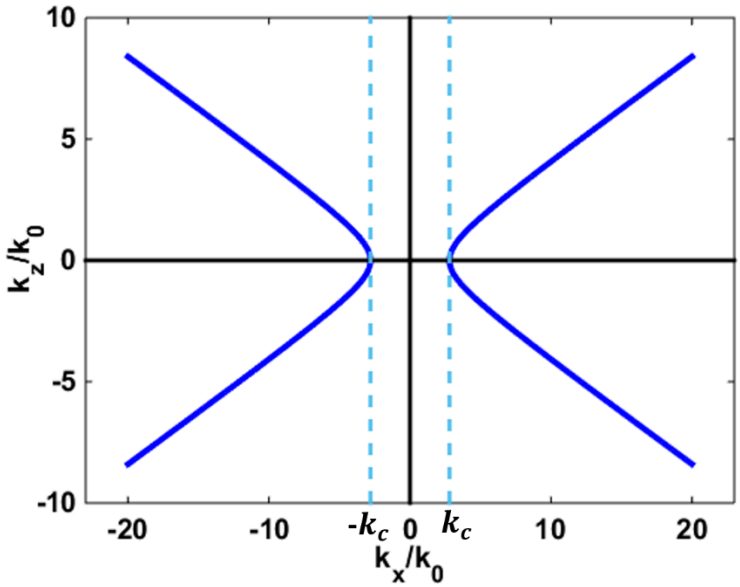

Figure SI-8. Dispersion relation of HMM at 700 nm. The HMM supports the propagation of modes with transverse wave-vectors larger than k_c.

5.2 Calculation of Purcell factors

In a planar system, when a dipole is placed at a distance d above a single or multi-layer film with a perpendicular (⊥) or parallel (∥) orientation to the interface, the corresponding Purcell F factor is experssed as the following:[1,2]

$$F_{\perp} = 1 - \eta_0 + \frac{3}{2}\eta_0 \mathrm{Re}\left[\int_0^{\infty} dk_x \frac{1}{k_z}\left(\frac{k_x}{\sqrt{\varepsilon_1}k_0}\right)^3 \left(1 + r_p e^{2ik_z d}\right)\right]$$

$$F_{\parallel} = 1 - \eta_0 + \frac{3}{4}\eta_0 \mathrm{Re}\left[\int_0^{\infty} dk_x \frac{1}{k_z}\frac{k_x}{\sqrt{\varepsilon_1}k_0}\left(1 + r_s e^{2ik_z d} + \frac{k_z^2}{\varepsilon_1 k_0^2}\left(1 - r_p e^{2ik_z d}\right)\right)\right]$$

Here, η_0 is the internal quantum efficiency of the emitter in free space and is assumed to be unity in this calculation. k_x and k_z are the components of the wave-vector along the x and z axis, respectively. k_0 is the free-space wave-vector. r_s and r_p are the reflection coefficients of the structure at the interface for an s and p polarized light, and are calculated using the transfer matrix method. ε_1 is the relative permittivity of the host media of the emitter and is unity in this calculation. The integrants in the above two equations refer to the normalized dissipated power spectra, which represents the energy emitted into different dissipation channels.

In the case of isotropic orientated emitters (2/3 contribution from parallel dipoles and 1/3 contribution from vertical dipoles), the average Purcell factor is calculated as:

$$F = \frac{1}{3}F_{\perp} + \frac{2}{3}F_{\parallel}$$

6. Al-doped Ag based transparent conductors

6.1 Mechanism of enhanced transmittance

One way to increase the transmittance (reduce reflection) of a thin metal film is to employ a dielectric-metal-dielectric (DMD) structure. The increased transmittance / reduced reflection is induced by multiple optical resonances within the dielectric layers. To show this, the net phase accumulation of each dielectric layer in the DMD structure of 45 nm TiO_2 / 7 nm Al-doped Ag / 40 nm TiO_2 / 100 nm MgF_2, which includes both the two reflection phase shifts from the two interfaces, and the propagation phase through the dielectric layer, is plotted in Figure SI-9. The resonant wavelengths (which correspond to a net phase accumulation of multiple of 2π radians) within each dielectric layer is denoted by circles in the plot. The transmittance is enhanced (reflection is suppressed) by the resonances within the dielectrics. The closely spaced multiple resonances contribute to the broadband enhancement of the transmission, and the suppressed reflection (denoted by the arrows).

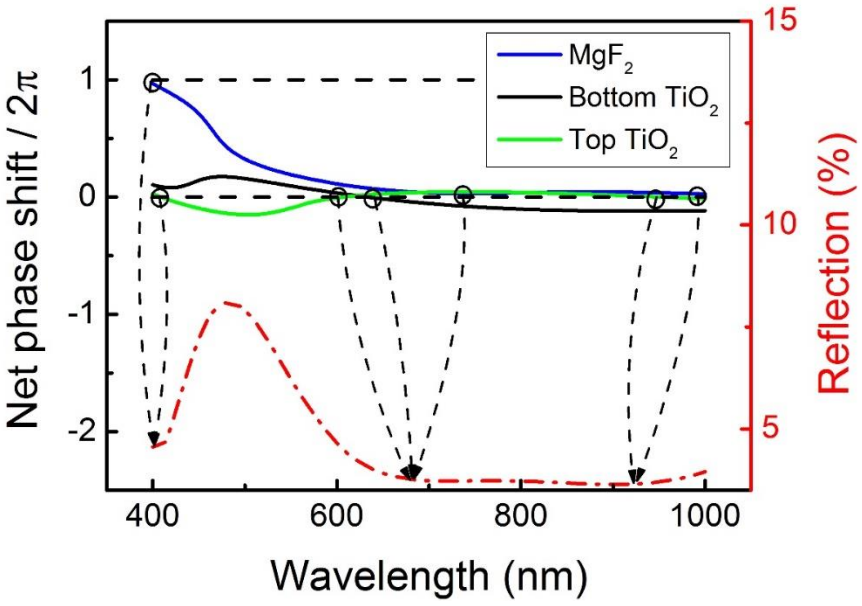

Figure SI-9. The net phase accumulation of each dielectric layer in the DMD transparent conductor consisting of 50 nm TiO_2/7 nm Al-doped Ag/40 nm TiO_2/100 nm MgF_2.

6.2 Optimized transmittance from DMD structures employing thicker metal films

The DMD design also applies to thicker Ag films. However, due to the increased absorption associated with thicker metal films, the optimized transmission is reduced. Figure SI-10 shows the simulated transmittance of optimized DMD structures based on thicker Al-doped Ag films. For a 10 nm Al-doped Ag, the optimized structure of 40 nm TiO_2 / 10 nm Al-doped Ag / 35 nm TiO_2 / 70 nm MgF_2 gives out an averaged transmittance of 87.4% from 400 nm to 1000 nm. The transmission is even lower for structures with 13 nm and 16 nm Al-doped Ag films (averaged transmittance of 80.1% and 71.7% respectively).

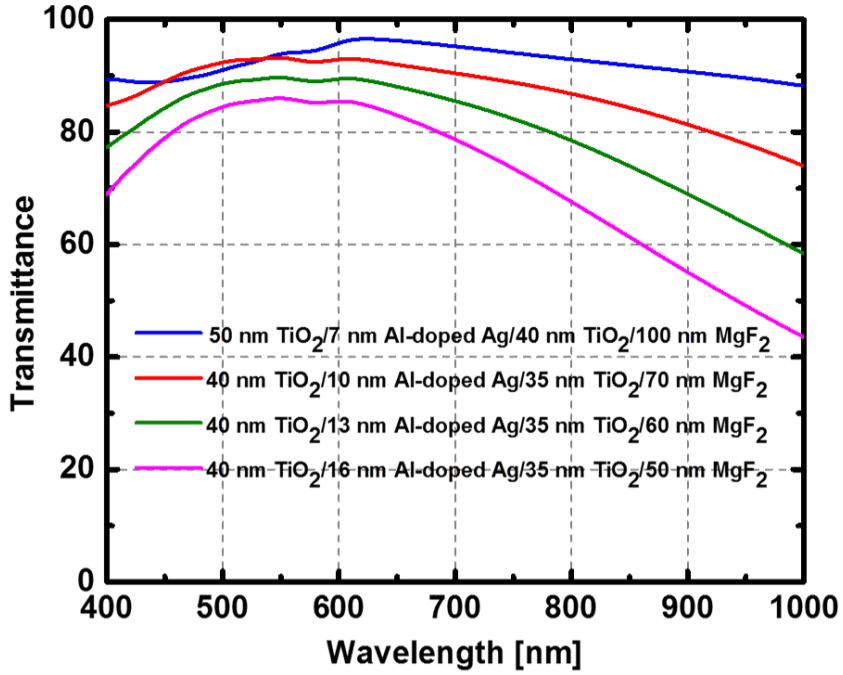

Figure SI-10. Simulated transmission spectra of transparent conductors with different Al-doped Ag layer thickness. For each Al-doped Ag layer thickness, the thicknesses of TiO_2 and MgF_2 layers are adjusted to achieve optimized transmission efficiency from 400 nm to 1000 nm.

Referneces:

[1] G.W.Ford and W.H. Weber, *Phys. Rep.* **1984**, *113*, *195*.

[2] W.L. Barnes, *J. Mod. Opt.* **1998**, *45*, *661*.